Published in Physical Review B 69, issue 125105, 1-5, 2003
which should be used for any reference to this work

Interplane coupling in the quasi-two-dimensional $1T$-TaS_2

M. Bovet,[1] S. van Smaalen,[2] H. Berger,[3] R. Gaal,[3] L. Forró,[3] L. Schlapbach,[1] and P. Aebi[1]
[1]*Département de Physique, Université de Fribourg, Pérolles, CH-1700 Fribourg, Switzerland*
[2]*Laboratory of Crystallography, University of Bayreuth, D-95440 Bayreuth, Germany*
[3] *Institut de Physique Appliquée, EPFL, CH-1015 Lausanne, Switzerland*

Density-functional band-structure calculations including atomic displacements in the charge-density wave phase have been performed for the layered $1T$-TaS_2. This quasi-two-dimensional material exhibits a charge-density wave extending in all three dimensions. We find that the topmost occupied Ta *d* band is localized in plane but strongly disperses perpendicular to the layers showing favorable nesting conditions in *z* direction. The calculations are compared to angle-resolved photoemission experiments and possible consequences on the temperature behavior of the resistivity are discussed.

Transition-metal dichalcogenides (TMCD's) are of strong interest since a long time because of their quasi-two-dimensional (2D) character with unique electronic properties and phase transitions.[1] $1T$-TaS_2 is a prototype for such layered materials with a rich phase diagram of charge-density waves (CDW's). The phase transitions give rise to strong changes in the resistivity [Fig. 1(a)]. It is characterized by a small anomaly at the phase transition at 350 K from an incommensurate CDW phase at high temperatures to a quasi-commensurate or nearly-commensurate (NC) phase at room temperature. Upon further lowering the temperature, a first-order transition takes place at 180 K into the commensurate (*C*) CDW phase together with an increase of the resistivity by an order of magnitude. The CDW formation is widespread in the TMDC family, whose simple form of the Fermi surface is given a high degree of 2D character.[1] Surprisingly, in $1T$-TaS_2, the CDW manifests itself also along the third dimension as shown again by a recent x-ray diffraction study.[2] Therefore, there has to be interaction between the layers. Furthermore, other unusual properties have been discovered in $1T$-TaS_2, notably a pseudogaped Fermi surface[3] and the absence of backfolding of bands according to the new Brillouin zones (BZ's) introduced by the periodic lattice distortion of the CDW.[4–6] The absence of backfolding effects is in apparent contradiction to non-self-consistent tight-binding calculations for a simplified structure describing the CDW phase performed by Smith *et al.*[7] This calculation shows that the reconstruction introduces three sub-band manifolds separated by gaps. Hence, the influence of the CDW should be manifest.

Here, we investigate the electronic properties of $1T$-TaS_2 using self-consistent full potential linearized augmented plane wave (FLAPW) calculations based on the experimental crystal structure using detailed refinement of the atomic positions by analyzing satellites up to high orders.[2] Furthermore, we compare our calculation to angle-resolved photoemission (ARPES) experiments.

The calculation shows that the CDW reconstruction induces drastic changes in the electronic structure confirming the three sub-band manifolds. However, we find that the reconstruction induces a *localization* of Ta-induced states *within* the plane and a *delocalization out* of plane. This behavior corresponds to an intriguing signature indicating a possible reason for the three-dimensional character of the CDW acting along the third dimension in these quasi-2D materials.

Bulk calculations have been done using the WIEN package[8] implementing the FLAPW method within the framework of density-functional theory (DFT). For the exchange-correlation potential the generalized gradient approximation was used.[9] The ARPES energy distribution curves (EDC's) have been collected at room temperature (RT) in a modified VG ESCALAB Mk II spectrometer using monochromatized He Iα ($h\nu = 21.2$ eV) photons.[10] The sequential motorized sample rotation has been outlined elsewhere.[11] The energy and angular resolution was 20 meV and 0.5°, respectively. Pure $1T$-TaS_2 samples were prepared by vapor transport[12,13] and cleaved *in situ* at pressures in the lower 10^{-10} mbar region. Cleanness has been checked by x-ray-photoelectron spectroscopy and crystallinity by low-energy electron diffraction (LEED). Well-defined LEED superspots confirmed the presence of the CDW-induced reconstruction. X-ray-photoelectron diffraction was used to determine the sample orientation *in situ* with an accuracy of better than 0.5°.

We first consider the morphology of the different phases. The *C*-phase superstructure below 180 K is characterized by star-shaped clusters of 13 atoms in the Ta plane and is associated with a high resistivity. The RT state is described by the NC phase, with hexagonally shaped domains of ≈ 70 Å diameter, where the structure within the domains is that of the *C* phase. It has a smaller resistivity with a semiconducting temperature dependence. Our calculations are based on the recent structure determination of the NC phase by Spijkerman *et al.*[2] For the band structure calculations a lattice periodic structure is required. Therefore, an approximate commensurate ($\sqrt{13}\times\sqrt{13}\times 3$) superstructure was derived from the refined structural coordinates of the incommensurate structure of the NC phase [Fig. 1(b)]. The supercell[14] (space group 147 $P\bar{3}$) shown in Fig. 1(b) is built by three sandwiches, each made of a Ta layer surrounded by two S planes. Lattice parameters are $a_0 = b_0 = 12.129$ Å and c_0

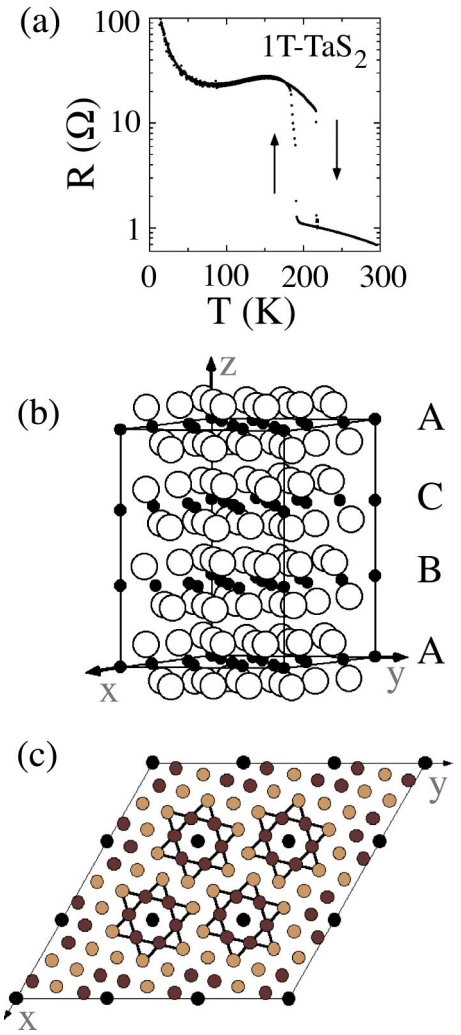

FIG. 1. In-plane resistance and structure of $1T$-TaS_2. (a) As measured on our sample. (b) Trigonal unit cell as derived from x-ray scattering measurements (see Ref. 2). Ionic radii have been used to plot Ta (black) and S (white) atoms. Sandwiches B and C result from the IC regions (see Ref. 2). (c) (3×3) Ta plane at $z\approx0$ (sandwich A) with the ''Stars of David'' containing 13 atoms: 12 neighbors displaced in direction of the star-centered, locked-in atom.

$=17.667$ Å. Most significant displacements are in plane for the Ta atoms, and out of plane for the sulfur atoms, resulting in a swelling out of S layers around Ta stars. In Fig. 1(c), inequivalent Ta atoms of the Ta [0001] plane (3×3 unit cells are shown) around $z=0$ are plotted with different shadings, thus displaying the clustering or the ''stars of David.''[15] The clusters of 13 Ta atoms consist of a central Ta atom, six equivalent nearest neighbors (N's) and six next-nearest neighbors (NN's) within one plane. The other two sandwiches at $z=1/3$ and 2/3 [Fig. 1(b)], equivalent to each other by inversion symmetry, contain only heavily distorted clusters because of the commensurate approximation. Since we are interested in the influence of the star formation, we extracted the first ($z\approx0$) sandwich for the calculation. Together with the symmetry of space group 147 ($P\bar{3}$) this results in a total of 39 atoms per unit cell, 13 Ta, and 26 S. The c parameter is 5.889 Å (one third of $c_0=17.667$ Å). In the absence of known parameters for the true structure in the C phase, this unit cell is used as an input for our calculation[17] to study the effect of the CDW on the electronic structure. The *undistorted* structure, i.e., the CdI_2-type structure with Ta planes arranged in a hexagonal lattice, was also computed for comparison. This structure has space group $P\bar{3}m1$ with lattice parameters $a_0=b_0=3.365$ Å and $c_0=5.853$ Å, and it contains three crystallographically independent atoms in the unit cell (one Ta and two S). This calculation[18] is much less time consuming than the one for the superstructure. The results are shown in Fig. 2(a). In the band structure of the unreconstructed plane (open circles), the well-known Ta derived d band[19] strongly disperses along Γ-M-K-Γ and A-L. However, it is localized (nondispersing) between Γ-A, pointing to no significant interaction of the Ta $5d$ electrons near the Fermi energy (E_F) along the z direction. Below -0.8 eV, the valence-band part is occupied by the S-derived p bands having a small indirect overlap with the Ta bands.

Figure 2(b) shows the relation between the hexagonal bulk and surface BZ's. The band structure of the superstructure has been computed employing the same k points, according to the correspondence between the *unreconstructed* and *reconstructed* BZ's [see Fig. 2(c)]. The result for the distorted structure [dots in Fig. 2(a)] exhibits a localized uppermost band along Γ-M-K-Γ at ≈-0.27 eV, with a dramatic Γ-A dispersion, followed by a small modulation from A to L. This band has mostly dz^2 character. Just below the dispersionless band, six sub-bands (having Ta d character) appear with a larger bandwidth. The six sub-bands are close to each other (in energy) at Γ [Fig. 2(a)]. While going towards M, they first spread out, then close again before spreading out again reaching M. The narrowing always marks the passage close to a Γ point of the reconstructed BZ [Fig. 2(c)]. The same characteristic behavior is observed along M-K. The density of states (DOS) per atom highlights that the energy range between the Fermi energy and -0.27 eV is mostly occupied by electrons of the Ta locked-in atoms [black curve, and black atoms in Fig. 1(c)]. At higher binding energies, the DOS originates from the N's and then from the NN's and also from the locked-in atoms. The complete energy range is slightly hybridized with electrons from the sulfur. Hence, the unreconstructed Ta derived d band has split into seven bands and, in accordance with the simple ionic picture,[16] the top $5dz^2$ band is occupied by the electron of the locked-in Ta atoms. The interaction of the layers indicated by the Γ-A dispersion cannot be explained by direct overlap of Ta orbitals since Ta interlayer distance is too large, it has to be mediated by the S atoms bulging out. This mediation is in line with the slight admixture of S character in the dispersing band along Γ-A.

Theoretical evidence of the seven Ta sub-bands has not been clearly confirmed by any experiment, although recent high-resolution ARPES measurements found six different peaks at $\bar{\Gamma}$ in an energy range down to 1 eV below E_F at low temperature.[20] Figure 3 shows the ARPES EDC's in the NC state along the surface direction $\bar{\Gamma}$-$\bar{M}$, thus probing the ΓALM plane of the bulk BZ. The experimental data has

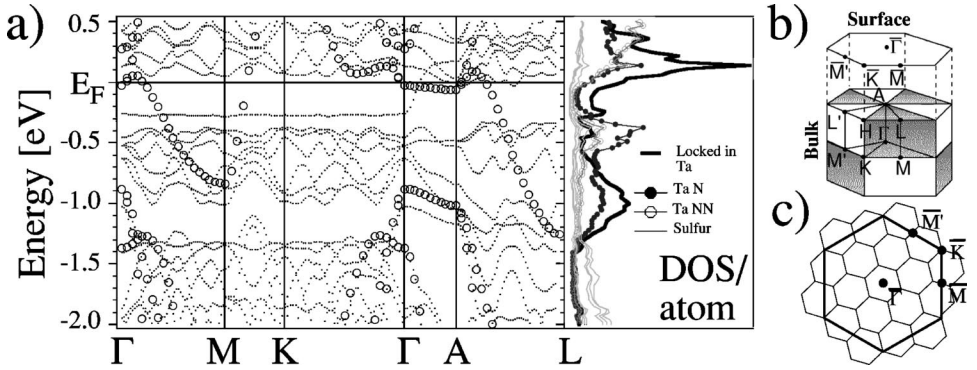

FIG. 2. Band structure calculations for *k* points along high symmetry directions within the unreconstructed BZ. (a) Superposition of both, the *unreconstructed* (open circles) and the CDW, *reconstructed* (dots) cases, followed by the density of states (DOS) per atom. (b) Surface and bulk BZ's. (c) *Reconstructed* (thin lines)-*unreconstructed* (thick lines) surface BZ's correspondence. The *reconstructed* BZ is rotated by 13.9° with respect to the *unreconstructed* one.

been divided by the Fermi-Dirac distribution in order to emphasize states around the Fermi level. In fact, ARPES is a surface sensitive technique, but we here only concentrate to relate our bulk calculations to the experiment. The simulation (right side) was obtained from the DFT calculation of the undistorted structure.[21] No photoemission matrix elements were included; they might explain the absence of bands in the lower right part of the ARPES EDC, while they appear in the DFT case. We note that the width of the calculated band is closer to the dispersion along *A*-*L* than to the one along Γ-*M* in Fig. 2(a). This is a consequence of the choice of parameters used to approximate the final state.[21] Nevertheless, the experimental spectral weight is well reproduced. Most importantly, the influence of the CDW induced new BZ's is not observed,[4–6] although at RT in the NC phase domains of ≈ 70 Å size exist with a structure corresponding to the *C* phase.[23,2]

However, very recently Voit *et al.*[22] have modeled the spectral weight distribution of tight-binding electrons in a solid with competing periodic potentials as in the case of the CDW superstructures. They show that the dispersion of the eigenvalues (band structure) follows the *reconstructed* BZ's, but the spectral weight (proportional to the photoemission intensity) is concentrated along the extended zone

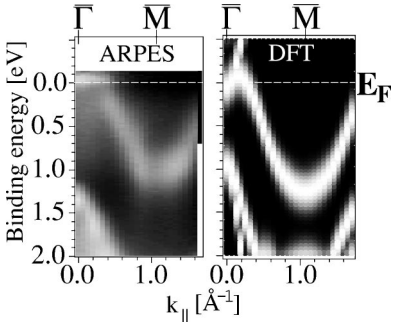

FIG. 3. Experimental (ARPES) and simulated (DFT) EDC's along $\bar{\Gamma}$-$\bar{M}$ of 1*T*-TaS_2. The experimental data has been divided by the appropriate Fermi-Dirac distribution in order to emphasize states around the Fermi level and then plotted with respect to $k_\parallel$. The simulation does not consider the CDW-induced reconstruction.

scheme dispersion of the nonreconstructed BZ. Figure 3 strongly suggests that the quasi-2D 1*T*-TaS_2 follows this behavior.

We now discuss the particular dispersion behavior of the band structure in the presence of the CDW [Fig. 2(a)]. The topmost occupied band (locked-in Ta atom) along Γ-*M*-*K*-Γ is strongly localized in plane and delocalized out of plane (Γ-*A*), as a consequence of the star formation. Up to now, nesting properties have been searched in plane, as the Fermi surface was supposed to be quasi 2D. As a matter of fact, from x-ray scattering, we know that the NC supercell has a *c* component equal to $3c_0$ or, in other words, that the modulation wave vector has a component of 1/3 in the *z* direction of the reciprocal space. In Ref. 2, that stacking period is explained by the S modulation and a corresponding optimized arrangement, in order to reach a maximum packing density. We address here the question of a *z*-nested Fermi surface with electron-phonon coupling, then possibly related to a Peierls instability and the fact that our quasi 2D-system has a CDW running also along the third dimension. Consequently the *z* part of the wave vector of the CDW, $\vec{q}_{CDW}$, should correspond to two times the Fermi wave vector $\vec{k}_F$. Ta atoms at the corners of the reconstructed unit cell in Fig. 1(b) form chains. Their *z* coordinates in each sandwich have been compared in Fig. 4(a) to the respective multiple of one third, thus leading to a plot of their vertical displacements with respect to an *unreconstructed* case, in fractional units of the unit cell. It clearly shows that the modulation of the corner atoms (black dots) ($\approx 0.8\%$ of c_0) is stronger than for the chains containing the neighbors. This experimental periodicity[2] corresponds to q_{CDW}. It is interesting now to place $\vec{q}_{CDW}$ into the calculated [Fig. 2(a)] band structure. The comparison is shown in Fig. 4(b). Although q_{CDW} appears slightly bigger than $2k_F$, the agreement is surprizingly good. A similar behavior is expected over the complete Fermi surface since along Γ-*A*, the uppermost dispersive band shows clearly a strong dispersion from the middle of the BZ to its border, but the in-plane dispersion [Fig. 2(a) is completely localized (Γ-*M*-*K*-Γ) or very weakly dispersive (*A*-*L*)], giving us a quasi 1D system.

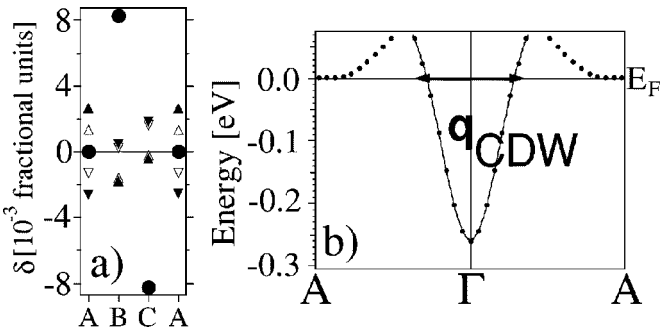

FIG. 4. Peierls distortion and nesting vector. (a) Vertical atomic displacements (δ) of the Ta atoms in each sandwich of the unit cell of Fig. 1(b). *N*'s and NN's are divided in up and down atoms, i.e., in sandwich A, slightly above, respectively, below $z=0$. Locked-in atoms (plain circles) are stronger shifted than the *N*'s (plain triangles) and NN's (empty triangles). (b) Estimated nesting vector along Γ-*A*.

Introduction of the complete unit cell of Fig. 1(b) in the calculation might consequently open a small gap, resulting in the band structure of a semiconductor, in good agreement with the temperature behavior or the resistivity [Fig. 1(a)] in the NC phase.[16] Consequently, the semiconductorlike temperature behavior of the resistivity between 350 K and 180 K would be a feature of the interplane electron-phonon coupling.

A specific feature of this system seems to be that many bands exist close to the Fermi level on the unoccupied side. And, at RT (ARPES in Fig. 3), a localized band seems to be occupied above the Fermi level, i.e., occupied thermally. As a consequence, the thermal occupation of these bands probably plays an important role for the resistivity of the 1*T*-TaS_2 and also for the number of charge carriers available. By lowering *T* less carriers are available and screening might become therefore less efficient. Then, at some point the system undergoes the Mott transition[16] allowing to lower even more the energy of the localized band of the locked-in Ta atom, developing into the lower Hubbard band. Close to, but below the transition temperature the resistivity has a metallic temperature behavior. A possible explanation could be the presence of midgap states[24] derived from bands of the kind seen in Fig. 2(a) along *A*-*L* at E_F. Such states would also explain the finite density of states in the gap observed by Dardel *et al.*,[12] thus leaving a pseudogap.

In conclusion, we have performed a DFT band structure calculation including effects of the atomic displacements corresponding to the CDW as extracted from the $(\sqrt{13}\times\sqrt{13}\times 3)$ unit cell deduced from x-ray diffraction[2] at RT. The particular spectral weight distribution of two competing potentials as described by Voit *et al.*[22] connects the calculated EDC's to the experimental photoemission intensities. The strong dispersion of the uppermost Ta dz^2 band along Γ-*A* has been related to the CDW induced interplane atomic displacements of the Tantalum chains including CDW locked-in atoms. Along these chains, supported by the particular stacking of the sandwiches at RT, the CDW would definitely open a gap in all the BZ, thus being consistent with the semiconducting behavior of the resistivity between 350 K and 180 K. Furthermore, the paradoxal metallic temperature behavior of the resistivity below 180 K (below the Mott transition) could be a consequence of remaining midgap states. Finally, the CDW, commonly described as acting in the Ta plane, appears to induce interaction perpendicular to the layers via hybridization of Ta and S states, by bulging out of S atoms around the star centers.

Skillful technical assistance was provided by E. Mooser, O. Raetzo, R. Schmid, Ch. Neururer, and F. Bourqui. We are obliged to F. Mariotti and C. Daul who made possible the computation of the distorted unit cell and thank L. Benfatto, C. De Morais Smith, and D. Baeriswyl for fruitful discussions. This project had been supported by the Fonds National Suisse de la Recherche Scientifique.

[1] J.A. Wilson, F.J. Di Salvo, and S. Mahajan, Adv. Phys. **24**, 196 (1975).

[2] A. Spijkerman, Jan L. de Boer, Auke Meetsma, Gerrit A. Wiegers, and Sander van Smaalen, Phys. Rev. B **56**, 13 757 (1997).

[3] Th. Pillo, J. Hayoz, H. Berger, M. Grioni, L. Schlapbach, and P. Aebi, Phys. Rev. Lett. **83**, 3494 (1999).

[4] R. Claessen, B. Burandt, H. Carstensen, and M. Skibowski, Phys. Rev. B **41**, 8270 (1990).

[5] Th. Pillo, J. Hayoz, H. Berger, F. Lévy, P. Aebi, and L. Schlapbach, J. Electron Spectrosc. Relat. Phenom. **101-103**, 811 (1999).

[6] Th. Pillo, J. Hayoz, H. Berger, R. Fasel, L. Schlapbach, and P. Aebi, Phys. Rev. B **62**, 4277 (2000).

[7] N.V. Smith, S.D. Kevan, F.J. Di Salvo, J. Phys. C **18**, 3175 (1985).

[8] P. Blaha, K. Schwarz, and J. Luitz, Computer Code WIEN97, (Karlheinz Schwarz, Technical Universitt Wien, Austria, 1999).

[9] John P. Perdew, K. Burke, and M. Ernzerhof, Phys. Rev. Lett. **77**, 3865 (1996).

[10] Th. Pillo, L. Patthey, E. Boschung, J. Hayoz, P. Aebi, L. Schlapbach, J. Electron Spectrosc. Relat. Phenom. **97**, 243 (1998).

[11] P. Aebi, J. Osterwalder, P. Schwaller, L. Schlapbach, M. Shimoda, T. Mochiku, and K. Kadowaki, Phys. Rev. Lett. **72**, 2757 (1994).

[12] B. Dardel, M. Grioni, D. Malterre, P. Weibel, Y. Baer, and F. Lévy, Phys. Rev. B **45**, 1462 (1992).

[13] B. Dardel, M. Grioni, D. Malterre, P. Weibel, Y. Baer, and F. Lévy, Phys. Rev. B **46**, 7407 (1992).

[14] The approximation is in the $(\sqrt{13}\times\sqrt{13})$ part: the true superstructure of the NC phase is incommensurate with CDW vectors of (x, y, 1/3), and x and y being almost equal to multiples of 1/13.

[15] R. Brouwer and F. Jellinek, Physica B **99**, 51 (1980).

[16] P. Fazekas and E. Tosatti, Philos. Mag. B **39**, 229 (1979); P. Fazekas and E. Tosatti, Physica B **99**, 183 (1980).

[17] The plane-wave cutoff K_{MAX} was determined by $R_{MT}K_{MAX}=7$, 5 and during iterations to self-consistency, the irreducible BZ was sampled by 308 k points. The magnitude of the largest vector in

charge-density Fourier expansion was $G_{max}=12$. No spin-orbit coupling was considered.

[18] This lighter calculation was done with 134 k point in the irreducible BZ, a $G_{max}=14$ and a $R_{MT}K_{MAX}=8$. No spin-orbit coupling was considered.

[19] H.W. Myron and A.J. Freeman, Phys. Rev. B **11**, 2735 (1975).

[20] Th. Pillo, J. Hayoz, D. Naumović, H. Berger, L. Perfetti, L. Gavioli, A. Taleb-Ibrahimi, L. Schlapbach, and P. Aebi, Phys. Rev. B **64**, 245105 (2001).

[21] The photoemission final state was assumed to be free electron-like, with a work function of 3.5 eV and an inner potential of 13 eV. No attempts were done to optimize these parameters.

[22] J. Voit, L. Perfetti, F. Zwick, H. Berger, G. Margaritondo, G. Gruner, H. Hochst, and M. Grioni, Science **290**, 501 (2000).

[23] X.M. Wu and C.M. Lieber, Science **243**, 1703 (1989).

[24] J. Isa, T. Fukase, M. Sasaki, M. Koyano, N. Taniguchi, T. Kimura, Y. Isobe, and H. Negishi, J. Low Temp. Phys. **127**, 63 (2002).